This paper is available on line at http://www.mcponline.org

Proteomic Analysis of Extracellular ATP-Regulated Proteins Identifies ATP Synthase β-Subunit as a Novel Plant Cell Death Regulator*[S]

Stephen Chivasa‡¶, Daniel F. A. Tomé‡¶, John M. Hamilton‡, and Antoni R. Slabas‡§

Extracellular ATP is an important signal molecule required to cue plant growth and developmental programs, interactions with other organisms, and responses to environmental stimuli. The molecular targets mediating the physiological effects of extracellular ATP in plants have not yet been identified. We developed a well characterized experimental system that depletes *Arabidopsis* cell suspension culture extracellular ATP via treatment with the cell death-inducing mycotoxin fumonisin B1. This provided a platform for protein profile comparison between extracellular ATP-depleted cells and fumonisin B1-treated cells replenished with exogenous ATP, thus enabling the identification of proteins regulated by extracellular ATP signaling. Using two-dimensional difference in-gel electrophoresis and matrix-assisted laser desorption-time of flight MS analysis of microsomal membrane and total soluble protein fractions, we identified 26 distinct proteins whose gene expression is controlled by the level of extracellular ATP. An additional 48 proteins that responded to fumonisin B1 were unaffected by extracellular ATP levels, confirming that this mycotoxin has physiological effects on *Arabidopsis* that are independent of its ability to trigger extracellular ATP depletion. Molecular chaperones, cellular redox control enzymes, glycolytic enzymes, and components of the cellular protein degradation machinery were among the extracellular ATP-responsive proteins. A major category of proteins highly regulated by extracellular ATP were components of ATP metabolism enzymes. We selected one of these, the mitochondrial ATP synthase β-subunit, for further analysis using reverse genetics. Plants in which the gene for this protein was knocked out by insertion of a transfer-DNA sequence became resistant to fumonisin B1-induced cell death. Therefore, in addition to its function in mitochondrial oxidative phosphorylation, our study defines a new role for ATP synthase β-subunit as a pro-cell death protein. More significantly, this protein is a novel target for extracellular ATP in its function as a key negative regulator of plant cell death. ***Molecular & Cellular Proteomics 10: 10.1074/mcp.M110.003905, 1–13, 2011.***

ATP is a ubiquitous, energy-rich molecule of fundamental importance in living organisms. It is a key substrate and vital cofactor in many biochemical reactions and is thus conserved by all cells. However, in addition to its localization and functions inside cells, ATP is actively secreted to the extracellular matrix where it forms a halo around the external cell surface. The existence of this extracellular ATP (eATP)[1] has been reported in several organisms including bacteria (1), primitive eukaryotes (2), animals (3), and plants (4–6). This eATP is not wasted, but harnessed at the cell surface as a potent signaling molecule enabling cells to communicate with their neighbors and regulate crucial growth and developmental processes.

In animals, eATP is a crucial signal molecule in several physiological processes such as neurotransmission (7, 8), regulation of blood pressure (9), enhanced production of reactive oxygen species (ROS) (10), protein translocation (11), and apoptosis (12). Extracellular ATP signal perception at the animal cell surface is mediated by P2X and P2Y receptors, which bind ATP extracellularly and recruit intracellular second messengers (13, 14). P2X receptors are ligand-gated ion channels that provide extracellular Ca^{2+} a corridor for cell entry after binding eATP, facilitating a surge in cytosolic [Ca^{2+}] that is essential in activating down-stream signaling. P2Y receptors transduce the eATP signal by marshalling heteromeric G-proteins on the cytosolic face of the plasma membrane and activating appropriate downstream effectors.

Although eATP exists in plants, homologous P2X/P2Y receptors for eATP signal perception have not yet been identified, even in plant species with fully sequenced genomes. Notwithstanding the obscurity of plant eATP signal sensors, some of the key downstream messengers recruited by eATP-mediated signaling are known. For example, eATP triggers a surge in cytosolic Ca^{2+} concentration (15–17) and a heightened production of nitric oxide (18–20) and reactive oxygen

From the ‡School of Biological and Biomedical Sciences, Durham University, Durham DH1 3LE, United Kingdom

Received August 3, 2010, and in revised form, November 24, 2010
Published, MCP Papers in Press, December 14, 2010, DOI 10.1074/mcp.M110.003905

[1] The abbreviations used are: eATP, extracellular ATP; FB1, fumonisin B1; ROS, reactive oxygen species; TSP, total soluble protein.

species (17, 21, 22). Altering eATP levels is attended by activation of plant gene expression (16, 21) and changes in protein abundance (5, 23), indicating that eATP-mediated signaling impacts on plant physiology. Indeed eATP has been demonstrated to regulate plant growth (20, 24–26), gravitropic responses (27), xenobiotic resistance (4), plant-symbiont interactions (28), and plant-pathogen interactions (23, 29). However, the mechanism by which eATP regulates these processes remains unclear, largely because the eATP signal sensors and downstream signal regulatory genes and proteins have not been identified.

We previously reported that eATP plays a central regulatory role in plant cell death processes (5). Therefore, an understanding of the signaling components galvanized by eATP in cell death regulation might serve a useful purpose in providing mechanistic detail of how eATP signals in plant physiological processes. We found that eATP-mediated signaling negatively regulates cell death as its removal by application of ATP-degrading enzymes to the apoplast activates plant cell death (5). Remarkably, fumonisin B1 (FB1), a pathogen-derived molecule that activates defense gene expression in *Arabidopsis* (30), commandeers this eATP-regulated signaling to trigger programmed cell death (5). FB1 is a mycotoxin secreted by fungi in the genus *Fusarium* and initiates programmed cell death in both animal and plant cells (31, 32). In *Arabidopsis*, FB1 inaugurates cell death by inactivating eATP-mediated signaling via triggering a drastic collapse in the levels of eATP (5). FB1-induced *Arabidopsis* programmed cell death is dependent on the plant signaling hormone salicylic acid (33), which is a key regulator of eATP levels (29). Because concurrent application of FB1 and exogenous ATP to remedy the FB1-induced eATP deficit blocks death, FB1 and exogenous ATP treatments can therefore be used as probes to identify the key signal regulators downstream of eATP in cell death control. This is vital for achieving the global objective of elucidating the mechanism of eATP signaling in plant physiology.

Gel-based proteomic analyses have been previously applied to successfully identify the novel role of eATP in the regulation of plant defense gene expression and disease resistance (23, 29). We have now employed FB1 and ATP treatments together with two-dimensional difference in-gel electrophoresis (DIGE) and matrix-assisted laser desorption-time of flight MS (MALDI-TOF MS) to identify the changes in *Arabidopsis* protein profiles associated with a shift from normal to cell death-inception metabolism. Additional reverse genetic analyses enabled us to definitively identify a putative ATP synthase β-subunit as a target for eATP-mediated signaling with an unexpected function in the regulation of plant programmed cell death.

EXPERIMENTAL PROCEDURES

Plant Material and Growth Conditions—Cell suspension cultures of *Arabidopsis thaliana* var. Landsberg erecta (34) were grown at 22 °C under a 16 h photoperiod (100 μmol/m^2/s) regimen. Cell cultures were used for experiments in mid-exponential growth phase (3–4 days postsubculturing). Soil grown-plants were incubated in a growth chamber with a 16 h photoperiod (100–120 μmol.m^{-2}.s^{-1}) maintained at 20 °C during the light phase and 15 °C during the dark phase. Plants were used for experiments 4–5 weeks following sowing.

Cell Culture Treatment—Stock solutions of FB1 (Sigma, Haverhill, UK) were prepared in 70% methanol and filter-sterilized before using to treat cell cultures. Mock treatments were performed with an equivalent dilution of 70% methanol. Stocks of filter-sterilized 100 mM ATP, pH 6.5 (adjusted with KOH) were prepared fresh every time. Samples for proteomic analysis were prepared by treating 3 days old *Arabidopsis* cell cultures adjusted to a cell density of 5% (w/v) in a 100 ml culture volume. One set of cultures (FB1) was treated with 1 μM FB1 at the beginning of the experiment, whereas the second set of cultures (FB1+ATP) was similarly treated with FB1, but 1 mM ATP was added 40 h later. The controls were mock-treated with methanol, the carrier solution for FB1. Each treatment had 4 independent biological replicates. The cells were harvested 48 h following the start of the experiment and frozen in liquid nitrogen.

Protein Sample Preparation—Cells were pulverised at 4 °C in a homogenization buffer (1 mM EDTA/10 mM Tris-HCl, pH 8.0) using a French Press (Constant systems Ltd., Warwick, UK) and the homogenate centrifuged (20,000 × *g*, 30 min, 4 °C). The supernatant, containing microsomal membranes and the total soluble protein fraction, was centrifuged (100,000 × *g*, 1 h, 4 °C) to separate these fractions. Total soluble protein (TSP) was recovered from the supernatant by precipitation (80% [v/v] acetone, −20 °C, 12 h) and extracted from the precipitate with a protein solubilization solution (9 M urea, 2 M thiourea, 4%[w/v] CHAPS). The microsomal membrane pellets were washed three times with homogenization buffer and protein extracted using the protein solubilization solution.

Protein Labeling and Gel Electrophoresis—Protein samples from four biological replicates of each treatment were labeled with CyDyes (GE Healthcare, Buckinghamshire, UK) as described before (35). Each biological replicate sample was split into two and one labeled with Cy3 and the other with Cy5 in a dye swap experimental design to preclude dye-specific artifacts (36). The pooled standard consisting of equal amounts of all the samples was labeled with Cy2. Protein mixtures containing 12.5 μg each of Cy3-and Cy5-labeled samples plus the Cy2-labeled pooled standard were resolved in 24 cm linear gradient pI 4–7 IPG strips for 70kVh as previously described (35). Second dimension separation was performed on an Ettan DALT Twelve System (GE Healthcare, Buckinghamshire, UK) in custom made 10–20% gradient polyacrylamide gels cast using the automated 2DE Optimizer gel caster (NextGen sciences, Cambridge, UK). Following resolution, the gels were immediately scanned using a Typhoon 9400 variable mode imager (GE Healthcare, Buckinghamshire, UK).

Image Analysis—Gel images were analyzed using DeCyder Differential Analysis Software version 6.5 (GE Healthcare, Buckinghamshire, UK) as described previously (35). Briefly, four biological and two technical replicates (from the dye-swap) comprised a total of 8 images per treatment. Spot detection, quantification and normalization of spot volume against the internal standard were performed automatically using the Differential In-Gel analysis module with estimated number of spots set to 5000. The Biological Variation Analysis module was used for spot matching and differential protein analysis. Matched spots were manually checked between gels to minimize false spot matching and exclude spot artifacts. The software automatically generated a ratio of sample spot volume to the pooled standard spot volume and normalized these ratios across all gels to generate standardized spot abundance values. The standardized spot abundance

values from the four biological replicates and two technical replicates were then averaged and the means subjected to Student's *t* test to check for statistically significant differences. Only manually inspected spots present in all replicate gels and displaying a significant ($p \leq 0.05$) FB1-induced change in abundance of a minimum of 20% (TSP) or 50% (microsomal protein) were selected for further analyses. The response of these spots to ATP added after FB1 was analyzed by statistical comparison of FB1+ATP average with FB1 only average. Only spots with an average standardized abundance that significantly ($p \leq 0.05$) shifted from the FB1 treatment average in response to the FB1+ATP treatment were selected for further analyses as ATP-responsive proteins. Probability values associated with the comparison of means were calculated using Student's *t* test.

MALDI-TOf MS Protein Identification—Preparative gels for protein identification loaded with 200 μg of unlabeled protein were stained with Sypro Ruby™ total protein stain (Genomic Solutions, Huntington, UK) according to the manufacturer's instructions. Differentially expressed spots were robotically excised using a ProPick Work station (Genomic Solutions, Huntington, UK) for identification by MALDI-TOF using a Voyager DE-STR Biospectrometry work station (Applied Biosystems, Warrington, Cheshire, UK) as described previously (37). Briefly, spot plugs of 2.0 mm diameter were digested with modified trypsin (Promega, Madison, WI) in a ProGest work station (Genomic Solutions, Huntington, UK) using the standard overnight digestion protocol supplied with the instrument. A total of 0.5 μl of each digest was spotted together with 0.5 μl of a saturated solution of α-cyano-4-hydroxycinnamic acid matrix directly onto a MALDI target plate using an Applied Biosystems Symbiot robot (Boston, MA). Instrument calibration was carried out for each sample using PE Sequazyme calibration mixture I (containing des-Arg-bradykinin, angiotensin I, Glu-fibrinopeptide B, and neurotensin). After each spot's spectra were acquired, automated peak detection, peak de-isotoping and noise reduction was carried out using Applied Biosystems Data Explorer 2.1.0 to generate peak mass tables. Trypsin peptide peaks (842.5 + 2211.1) were used as internal calibrants and were excluded from database searches. The peptide mass fingerprint for each spot was used to search *Viridiplantae* (green plants) sequences in the nonredundant NCBInr database version 20070713 (5269953 sequences; 1825351362 residues) using the Mascot 4.0 search engine (Matrix Science, London, UK). The following search parameters were used: peptide mass tolerance: ± 50 ppm, maximum number of missed cleavages: 1, fixed modifications: carbamidomethylation of cysteine residues, variable modifications: oxidation of methionine residues. The Mascot software probability-based MOWSE score cut-off for a significant ($p \leq 0.05$) positive protein identification of 71 was applied. Where more than one database entry was obtained from a single spot, the spots were excluded because it was impossible to know which of the proteins in the mixture were differentially regulated.

RNA Analysis and PCR Reactions—Total RNA was extracted using RNeasy Plant kit (Qiagen, Crawley, UK), with on-column DNase treatment, according to the manufacturer's instructions. First-strand cDNA synthesis was performed as previously described (35) using oligo-$(dT)_{15}$ (Progema, Southampton, UK), 3 μg of total RNA and SuperScript III reverse transcriptase (Invitrogen, Paisley, UK). For PCR reactions, the following primer pairs were used: *ATP SYNTHASE β-SUBUNIT* (At5g08690) 5′-TCCACACACCCACTCATGGCG-3′ and 5′-TCACAATGCCTCAGCAGACAACC-3′; *ACTIN 2* (At3g18780) 5′-GGATCGGTGGTTCCATTCTTG-3′ and 5′-AGAGTTGTCACACACAAGTG-3′, *SEN1* (At4g35770) 5′-TTAAAATTCCTACGTCAGTACCAG-3′ and 5′-TCTCTGTCCAAGCGACGTATCC-3′.

Cell Death Assays—Discs of 8 mm diameter were cored from leaves of 4-week-old plants and floated on 10 μM FB1 solutions in triplicate Petri-dishes. Each replicate had 10 leaf discs each originating from one of 10 replicate plants. The discs were incubated in the dark for 48 h to allow uptake of FB1 prior to the onset of cell death. After the dark incubation, the discs were placed under a 16 h photoperiod regime and the conductivity of the underlying solution measured at 24 h intervals using a Jenway conductivity meter (Jenway Ltd., Felsted, UK). In addition, 10 μM FB1 was also infiltrated into the apoplast of attached leaves from the abaxial surface using a syringe without a needle. Symptom development was visually monitored and photographs taken 4 days following infiltration.

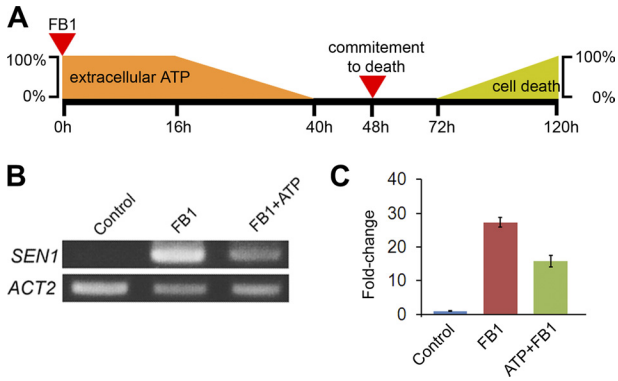

FIG. 1. **Schematic representation of FB1-induced events and the effects of exogenous ATP.** *A*, addition of FB1 to cell cultures triggers eATP depletion commencing ~16 h later and disappearing below detection at ~40 h. Cells irreversibly commit to die at ~48 h and cell death starts at ~72 h. Exogenous ATP added at 40 h attenuates FB1-induced signaling and gene expression, thereby blocking cell death. Note that the decline of eATP from 100–0% and the increase of cell death from 0–100% do not progress at rates indicated by the gradients on the diagram. *B*, induction by FB1 of a cell death marker, *senescence-associated 1* (*SEN1*), is attenuated by exogenous ATP. Samples for RT-PCR were harvested at 42 h. *Actin-2* (*ACT2*) was used as a constitutive reference control. *C*, densitometric analysis of *SEN1* PCR bands from (*B*) expressed as fold-change relative to the control sample. Data and error bars are means ± se ($n = 3$).

RESULTS

Establishing the Experimental System—To identify eATP-regulated proteins with a putative function in cell death regulation, we used *Arabidopsis* cell cultures treated with FB1 or FB1+ATP. FB1 inactivates eATP-mediated signaling by triggering removal of the input signal (eATP), thereby initiating cell death (5). Exogenous ATP supplied back to the FB1-treated cultures rescues the cells from death, most probably by re-establishing the eATP-mediated signaling. Thus, exogenous ATP treatment can be used as a filter to identify the subset of FB1-induced genes/proteins whose expression and abundance is altered in response to the specific depletion of eATP. We used the cell death marker *SEN1* (At4g35770), a gene activated during senescence-associated programmed cell death (38), to validate the utility of the exogenous ATP filter in this experimental system. FB1 treatment up-regulated *SEN1* expression, but, in accordance with its ability to blockade FB1-induced cell death (5), exogenous ATP attenuated the response of this gene to FB1 treatment (Fig. 1). Because exogenous ATP effectively blocked FB1 effects at the transcript level, it is most likely that this is reflected at the protein

level as well. Therefore, a comparative analysis of protein profiles of mock-treated cultures with FB1- and FB1+ATP-treated cultures can reveal eATP-regulated proteins that mediate its physiological effects, including cell death control.

We have previously shown that exogenous ATP rescues cells from death if added concurrently with FB1 or any time up to ~40 h later, but fails to rescue the cells if added ~48 h or thereafter (5). Although 40 h coincides with the time when eATP levels have diminished below detection (5), these findings indicate that the cells' metabolism irreversibly commits to cell death at ~48 h, with cell death symptoms appearing ~24 h later (5). Therefore, we chose to perform proteomic analyses at the 48 h time point in order to detect the changes that switch normal metabolism to a death program, but that precede actual cell death. The timing of events triggered by FB1 addition to *Arabidopsis* cell cultures is illustrated schematically in Fig. 1.

Protein Gel Analysis and Protein Identification—Fractions enriched for total soluble protein (TSP) and microsomal membrane protein were prepared from *Arabidopsis* cell cultures exposed to FB1 or a combination of FB1+ATP treatments. In the latter, ATP was added to the cell cultures 40 h after FB1. Treated cells were harvested for protein extraction at the 48 h time point. Images of the protein gels revealed big differences in the profiles of TSP and microsomal membrane proteins (Fig. 2), indicating that analysis of the two separate fractions enabled the coverage of a wider range of proteins than would be achievable if only one of the protein fractions was targeted for analysis. As we used a gel-based approach, it is obvious that only a fraction of the membrane-associated proteins are represented in this study because highly hydrophobic proteins do not easily enter two-dimensional gels. However, this inadvertently helped to simplify the protein profile by reducing the number of proteins.

Quantitative analysis was performed using two-dimensional DIGE on four independent biological replicates of each treatment and two technical replicates of each sample. Average standardized spot volumes of the control and FB1 treatments were compared using Student's *t* test and the fold-change in protein abundance calculated by generating the ratio [FB1/control] for up-regulated spots or [control/FB1] for down-regulated spots (Tables I and II). To quantify the effects of ATP on FB1-induced changes in protein abundance, average spot volumes of the FB1 and FB1+ATP treatments were compared using the Student's *t* test and the ratio [FB1+ATP/FB1] or [FB1/FB1+ATP] generated for up-regulated or down-regulated spots, respectively (Tables I and II). The ratio of down-regulated spots is indicated by a minus sign in both Tables I and II.

Approximately 5000 features, including both authentic protein spots and some artifacts, were automatically detected on the pooled standard master gels. The majority of protein spots in both the TSP and microsomal protein fractions did not respond to FB1 treatment. The abundance of 145 protein

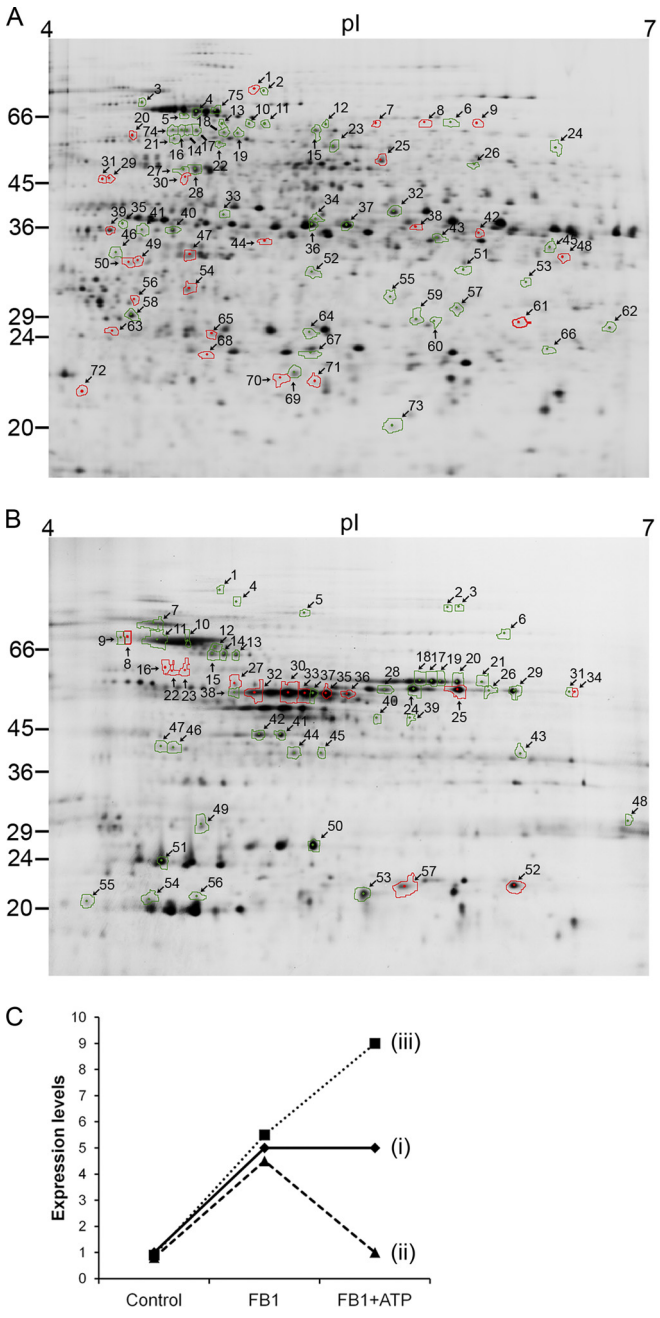

FIG. 2. **2-D DIGE analysis of *Arabidopsis* proteins and their response profile.** Total soluble protein (*A*) and microsomal membrane protein (*B*) fractions were analyzed by 2-D DIGE and protein spots responding to FB1 alone (*green boundary*) or to both FB1 and exogenous ATP (*red boundaries*) were identified by MALDI-TOF MS. *C*, protein response profiles: some proteins responded only to FB1 (*profile i*), and others to both FB1 and ATP (*profiles ii and iii*). Reciprocals of these profiles are also considered to belong to the same response group.

spots in the TSP fraction was significantly ($p \leq 0.05$) altered in response to FB1 treatment by at least 20%. Of these 145 TSP spots, only 75 were positively identified (Table I). The remaining 70 could not be positively identified - the majority being

TABLE I
TSP fraction proteins differentially expressed in response to FB1 and FB1+ATP

Spot	Gene locus	Protein name	Score[a]	Sequence coverage	Peptides[b]	FB1/Control		FB1+ATP/FB1	
						Ratio[c]	*p* value	Ratio[d]	*p* value[e]
				%					
Molecular chaperones									
3	At5g02500	heat shock cognate protein 70–1	85	31	15	1.21	2.2e-3	1.05	nss
4	At3g12580	heat shock protein 70 (HSP70)	146	36	24	1.22	3.6e-2	1.22	nss
10	At5g09590	heat shock protein 70 (Hsc70–5)	250	49	35	1.24	7.1e-3	−1.15	1.1e-2
14	At5g02500	heat shock cognate protein 70–1	89	28	20	1.24	1.3e-2	−1.13	nss
16	At5g02500	heat shock cognate protein 70–1	126	40	18	1.26	1.5e-2	−1.13	nss
17	At5g02500	heat shock cognate protein 70–1	123	33	20	1.36	3.3e-3	−1.10	nss
18	At3g12580	heat shock protein 70 (HSP70)	129	33	22	1.42	5.6e-5	−1.02	nss
19	At3g12580	heat shock protein 70 (HSP70)	80	19	13	1.52	3.0e-5	1.04	nss
20	At1g77510	protein disulfide isomerase-like	148	51	19	−1.26	1.5e-2	1.23	2.5e-2
21	At4g37910	mitochondrial heat shock protein 70–1	177	38	25	−1.26	9.5e-3	−1.19	nss
22	At3g12580	heat shock protein 70 (HSP70)	112	26	22	1.78	8.3e-5	−1.19	nss
29	At4g24190	heat shock 90.7 like protein	104	30	11	1.34	6.6e-4	−1.38	8.0e-4
30	At5g52640	heat shock protein AtHSP90.1	76	15	11	1.38	5.8e-6	−1.26	1.4e-2
31	At4g24190	heat shock 90.7 like protein	95	22	15	1.23	8.3e-3	−1.38	4.0e-4
39	At5g52640	heat shock protein AtHSP90.1	123	27	19	1.20	2.8e-2	−1.70	4.3e-3
57	At5g02500	heat shock cognate protein 70–1	83	18	15	−1.57	1.8e-3	−1.20	nss
69	At1g53540	17.6 kDa class I small heat shock protein	90	38	10	1.3	4.5e-3	−1.04	nss
74	At3g09440	heat shock cognate 70 kDa protein 3	97	32	21	1.25	3.1e-2	−1.22	nss
75	At3g12580	heat shock protein 70 (HSP70)	249	56	37	1.27	7.2e-3	1.16	1.1e-2
Glycolytic enzymes									
7	At1g70730	putative phosphoglucomutase	181	44	23	−1.41	2.5e-2	1.38	4.2e-2
8	At1g23190	putative phosphoglucomutase	169	37	21	−1.75	2.1e-4	1.73	2.1e-2
15	At3g08590	putative phosphoglycerate mutase	142	52	19	−1.22	2.3e-2	1.33	nss
38	At3g52930	fructose-bisphosphate aldolase	95	42	10	−1.21	2.5e-2	1.35	6.0e-3
42	At3g04120	GAPDH (C subunit)	104	45	16	−1.24	1.9e-2	1.68	8.0e-4
43	At3g04120	GAPDH (C subunit)	141	43	15	−1.22	9.1e-7	−1.06	nss
50	At1g79550	phosphoglycerate kinase (PGK)	124	62	19	−1.38	3.6e-3	−1.41	2.7e-3
51	At2g36460	fructose-bisphosphate aldolase	85	45	9	−1.44	9.4e-4	−1.08	nss
52	At3g52930	fructose-bisphosphate aldolase	146	57	14	−1.22	1.4e-2	−1.17	4.5e-2
65	At3g52930	fructose-bisphosphate aldolase	86	48	11	1.25	1.0e-2	−1.58	2.4e-3
Antioxidant enzymes									
6	At3g52880	monodehydroascorbate reductase	100	33	11	−1.53	1.2e-5	1.23	nss
49	At5g03630	monodehydroascorbate reductase	116	45	18	−1.49	2.8e-5	−1.26	1.5e-2
53	At5g16970	2-alkenal reductase (EC 1.3.1.74)	96	48	14	1.26	1.3e-3	−1.13	nss
67	At1g19570	dehydroascorbate reductase	109	66	10	−1.25	1.6e-4	−1.05	nss
71	At1g02930	glutathione transferase	114	38	11	1.53	2.9e-4	−1.58	9.0e-3
72	At5g42980	thioredoxin	99	72	11	−1.49	6.5e-4	−1.38	2.5e-2
Cytoskeleton-related proteins									
27	At1g04820	alpha tubulin isoform	135	45	16	−1.28	2.3e-2	1.33	nss
38	At1g04820	alpha tubulin isoform	178	47	15	−1.27	4.2e-2	1.30	nss
35	At3g60830	actin-related protein	84	33	9	−1.5	5.6e-3	−1.12	nss
64	At5g09810	actin 7	80	45	15	1.29	4.1e-4	1.10	nss
73	At5g59880	actin depolymerizing factor 3	111	75	12	−1.21	1.9e-3	1.08	nss
Protein degradation									
2	At2g30110	ubiquitin-activating enzyme (E1)	91	17	16	−1.33	1.9e-2	1.29	nss
59	At2g27020	20S proteasome subunit PAG1	117	39	14	1.21	5.6e-3	−1.13	nss
62	At3g22110	α-3 subunit of 20s proteasome	89	47	11	−1.36	1.5e-6	1.18	nss
63	At1g64520	regulatory particle non-ATPase 12a	116	51	15	1.20	2.7e-2	−1.45	8.7e-3
66	At3g60820	20S proteasome β-subunit PBF1	156	60	15	1.38	6.4e-4	−1.02	nss
Amino acid metabolism									
13	At5g53460	NADH-dependent glutamate synthase	130	41	16	1.52	9.9e-4	−1.14	nss
23	At3g58610	ketol-acid reductoisomerase	189	30	18	−1.29	1.7e-2	1.31	nss
24	At5g17920	cobalamin-independent methionine synthase	90	17	11	1.27	1.4e-2	−1.13	nss
36	At3g17820	glutamine synthetase	108	29	13	1.32	1.5e-4	1.20	nss
37	At3g17820	glutamine synthetase	219	76	27	1.47	9.6e-6	1.16	nss
47	At3g53580	diaminopimelate epimerase	153	57	21	−1.22	7.8e-4	−1.26	6.0e-4
Unclassified									
1	At1g79690	Nudix hydrolase homolog 3	74	39	12	−1.37	8.5e-3	1.52	4.6e-2
5	At5g03340	putative cell division cycle protein 48	80	26	16	1.18	4.8e-3	1.05	nss
9	At2g17980	ATSLY1 protein transporter	102	36	21	−1.5	1.9e-3	1.29	4.2e-2
11	At3g60750	putative transketolase	92	20	12	1.35	3.7e-3	−1.08	nss
12	At3g09840	cell division cycle protein	92	29	16	1.26	1.1e-2	1.09	nss
25	At4g13940	S-adenosyl-L-homocysteine hydrolase	125	46	21	1.35	2.7e-2	1.65	9.0e-3

TABLE I—*continued*

Spot	Gene locus	Protein name	Score[a]	Sequence coverage	Peptides[b]	FB1/Control		FB1+ATP/FB1	
						Ratio[c]	*p* value	Ratio[d]	*p* value[e]
				%					
26	At4g13430	Isopropyl malate isomerase large subunit 1	98	35	16	−1.24	1.5e-2	1.31	nss
32	At1g77120	alcohol dehydrogenase	81	24	9	−1.45	7.0e-3	1.56	nss
33	At5g08690	ATP synthase β-subunit	138	42	21	1.27	3.4e-5	−1.14	2.3e-2
34	At3g29360	putative UDP-glucose 6-dehydrogenase	162	58	28	1.27	1.7e-5	−1.05	nss
40	At1g62380	ACC oxidase	85	43	12	−1.59	2.7e-3	1.19	nss
41	At3g14990	thiazole monophosphate biosynthesis protein	95	45	19	−1.58	4.0e-5	1.15	nss
44	At1g03475	coproporphyrinogen III oxidase	140	46	18	−1.29	2.2e-2	1.32	5.6e-3
45	At5g08670	ATP synthase β-subunit	90	49	20	1.27	5.7e-3	−1.06	nss
46	At2g44060	late embryogenesis abundant family protein	137	61	21	1.28	1.3e-4	−1.13	2.4e-2
48	At3g18130	similarity to mammalian RACKs	111	46	14	−1.51	1.6e-2	1.88	1.1e-2
54	At4g34050	putative caffeoyl-CoA 3-O-methyltransferase	136	61	21	1.87	1.9e-6	−1.33	1.8e-3
55	Atmg01190	ATPase subunit 1	282	52	27	−1.21	3.0e-4	−1.19	3.3e-3
56	At4g13940	S-adenosyl-L-homocysteine hydrolase	82	38	10	1.29	6.0e-4	−1.20	1.1e-2
58	At4g13940	S-adenosyl-L-homocysteine hydrolase	137	57	17	1.22	5.1e-3	−1.26	nss
60	At2g21250	mannose 6-phosphate reductase	77	37	11	−1.48	24e-4	1.02	nss
61	At5g15650	reversibly glycosylated polypeptide-2	123	26	10	1.38	1.4e-2	−1.51	2.3e-2
68	At3g56090	ferritin 3 AtFER3	123	52	17	1.26	1.3e-2	−1.5	5.0e-3
70	At5g38480	general regulatory factor 3	108	34	12	1.25	9.2e-3	−1.3	1.5e-2

[a] Mowse score, for a significant ($p < 0.05$) positive protein identification, cut-off threshold was 71.

[b] Number of peptides matched to the protein sequence.

[c] Ratio represents fold-change of FB1 relative to the control treatment.

[d] Ratio represents fold-change of FB1+ATP relative to FB1 *i.e.* comparison of the FB1+ATP average with the FB1 average to check if ATP addition significantly altered protein response to FB1 alone.

[e] Probability value was replaced by nss when the difference between the treatments being compared was not statistically significant (*i.e.* *p* value >0.05).

low abundance spots, from which inadequate sample was present in the preparative gel to enable identification, whereas a few were in protein mixtures. Spots with protein mixtures were excluded because it was not possible to determine which of the proteins was changing in abundance in response to the treatments. A total of 83 protein spots significantly ($p \leq 0.05$) responded to FB1 by at least a 50% change in abundance in the microsomal membrane fraction. Only 57 of these were positively identified (Table II) whereas identification of the rest was similarly hindered by low abundance or existence as multiple protein mixtures on the gels. The total number of positively identified protein spots in both the TSP and microsomal membrane fractions was 132 (Tables I and II), but this represented 74 unique proteins. The redundancy revealed by the inequality between the number of protein spots and unique proteins arises from the existence of post-translationally modified polypeptides and an overlap of 13 proteins that were identified in both protein fractions. Additional data relating to protein identification is presented in supplemental Table 1 and supplemental Protein Mass Spectra.

The exogenous ATP filter revealed the subset of FB1-responsive proteins, which is regulated by the level of eATP. The response of 24 TSP spots and 16 microsomal membrane protein spots to FB1 was attenuated by exogenous ATP (Fig. 2*C profile ii*). These are the proteins most likely to mediate the physiological effects of eATP. A total of 26 unique proteins were in this category. However, the majority of the FB1-responsive proteins remained unaffected by exogenous ATP (Fig. 2*C profile i*), indicating that FB1 has other targets and physiological effects that are independent of its ability to trigger eATP depletion. A minority of the spots (eight spots) had their response to FB1 enhanced by the addition of exogenous ATP (Fig. 2*C profile iii*). This result suggests that FB1 and exogenous ATP activate common, but as yet uncharacterized, plant signaling cascades where a combination of the two compounds has a synergistic effect.

Classification of Differentially Expressed Proteins—The identified proteins were classified into several functional categories (Tables I and II). Molecular chaperones and heat shock proteins were highly represented in the data sets and they were largely up-regulated in response to FB1. Remarkably, exogenous ATP attenuated this heightened increase in molecular chaperones, indicating that FB1-induced depletion of eATP is the central cue for the deployment of this protein response. Many subunits of the ATP synthesis machinery were down-regulated by FB1 treatment, but again this response was dependent on the level of eATP because exogenous ATP impeded this response. Although the majority of spots in this category were from the mitochondrial ATP synthase, vacuolar and chloroplastic ATP synthase subunits were also identified. Several cellular redox control proteins were suppressed in response to FB1. These included a glutathione *S*-transferase, dehydroascorbate reductase, and thioredoxin. Curiously, exogenous ATP enhanced the suppression of these proteins, indicating that eATP depletion *per ser* is not the cue for this response. Central metabolic pathways, such as glycolysis and amino acid synthesis were also affected by

TABLE II
Microsomal proteins differentially expressed in response to FB1 and FB1+ATP

Spot	Gene locus	Protein name	Score[a]	Sequence coverage	Peptides[b]	FB1/Control		FB1+ATP/FB1	
						Ratio[c]	*p* value	Ratio[d]	*p* value[e]
				%					
Molecular chaperones									
1	At1g79930	high molecular weight heat shock protein	128	36	27	1.93	2.4e-7	−1.09	nss
5	At5g15450	chloroplast-targeted Hsp101 homologue	90	32	31	−1.59	3.5e-3	1.14	nss
7	At5g56030	heat shock protein 90 (HSP90)	218	39	36	1.78	1.1e-6	1.00	nss
8	At4g24280	chloroplast heat shock protein 70–1	74	21	15	2.19	4.5e-9	−1.20	9.7e-3
9	At4g24280	chloroplast heat shock protein 70–1	137	31	21	2.09	5.1e-7	−1.18	0.014
10	At5g02500	heat shock cognate protein 70–1	214	56	29	1.79	9.3e-7	−1.10	nss
11	At5g02500	heat shock cognate protein 70–1	187	48	27	2.13	2.3e-8	−1.08	nss
12	At3g12580	heat shock protein 70 (HSP70)	218	48	26	2.13	3.6e-7	−1.17	nss
15	At4g37910	mitochondrial heat shock protein 70–1	102	44	28	−1.54	2.3e-4	1.21	nss
16	At4g37910	mitochondrial heat shock protein 70–1	98	34	20	2.04	9.9e-5	−1.31	2.5e-2
22	At4g37910	mitochondrial heat shock protein 70–1	106	47	29	3.14	1.1e-5	−1.65	9.6e-3
23	At4g37910	mitochondrial heat shock protein 70–1	101	26	16	4.34	8.3e-8	−1.6	3.2e-3
46	At5g52640	heat shock protein AtHSP90.1	98	23	16	2.85	4.5e-5	−1.41	nss
47	At5g56010	heat shock protein 90 (HSP90)	85	27	14	2.87	3.8e-5	−1.43	nss
54	At4g25200	AtHSP23.6-mito	84	52	10	−2.29	1.4e-6	−1.03	nss
ATP synthesis machinery									
13	At1g78900	vacuolar ATP synthase subunit A	156	47	25	−1.80	7.0e-5	1.19	nss
14	At1g78900	vacuolar ATP synthase subunit A	192	39	22	−1.63	1.9e-4	1.19	nss
24	Atmg01190	ATPase subunit 1	207	41	20	−2.01	5.5e-6	1.30	4.1e-2
25	Atmg01190	ATPase subunit 1	213	51	27	−1.96	2.2e-6	1.28	nss
26	Atmg01190	ATPase subunit 1	235	60	29	−2.81	4.0e-6	1.29	nss
27	Atcg00120	ATPase CF1 α-subunit	216	37	20	−1.70	1.9e-4	1.29	3.4e-2
28	Atmg01190	ATPase subunit 1	164	35	16	−2.31	4.4e-8	1.17	nss
29	Atmg01190	ATPase subunit 1	207	51	24	−1.93	2.0e-5	1.26	nss
30	At5g08690	mitochondrial ATP synthase β-subunit	217	58	27	−1.88	4.1e-7	1.24	1.6e-2
31	Atmg01190	ATPase subunit 1	197	36	18	−1.69	5.9e-4	1.21	nss
32	At5g08690	mitochondrial ATP synthase β-subunit	248	63	28	−2.17	5.3e-8	1.23	1.4e-2
33	At5g08690	mitochondrial ATP synthase β-subunit	250	62	28	−1.86	8.2e-7	1.32	2.5e-2
34	Atmg01190	ATPase subunit 1	79	23	10	−1.69	8.3e-4	1.22	2.6e-2
35	At5g08690	mitochondrial ATP synthase β-subunit	251	64	25	−1.72	3.0e-5	1.34	2.9e-2
36	At5g08690	mitochondrial ATP synthase β-subunit	249	60	25	−1.74	2.9e-4	1.38	1.8e-2
37	At5g08690	mitochondrial ATP synthase β-subunit	217	58	27	−2.04	5.9e-6	1.28	nss
38	At5g08690	mitochondrial ATP synthase β-subunit	112	33	14	−1.78	1.8e-6	1.13	2.2e-2
39	At5g08690	mitochondrial ATP synthase β-subunit	206	55	27	3.07	1.6e-7	1.16	nss
50	At2g21870	unknown protein mitochondrial	137	65	19	−2.03	2.1e-5	1.23	nss
52	At5g13450	ATP synthase delta chain	185	63	18	−1.83	3.5e-6	1.23	3.4e-2
53	At5g08670	mitochondrial ATP synthase β-subunit	124	59	22	−1.7	3.2e-6	1.12	nss
56	At3g52300	ATP synthase D chain	212	83	20	−2.32	3.6e-6	−1.12	nss
57	At5g13450	ATP synthase delta chain	133	53	14	−1.68	8.6e-6	1.23	2.7e-2
Unclassified									
2	At1g56070	translation elongation factor 2-like	88	38	28	2.28	2.2e-5	1.04	nss
3	At1g56070	translation elongation factor 2-like	125	46	30	2.24	6.4e-9	1.09	nss
4	At3g09840	cell division cycle protein	91	14	14	3.35	9.4e-9	−1.09	nss
6	At5g17920	cobalamin-independent methionine synthase	88	37	21	5.18	9.1e-10	1.11	nss
17	At3g02090	metalloendopeptidase (MPPBETA)	137	37	15	−1.92	9.4e-5	1.21	nss
18	At3g02090	metalloendopeptidase (MPPBETA)	209	59	26	−1.94	1.4e-5	1.19	nss
19	At3g02090	metalloendopeptidase (MPPBETA)	184	57	22	−1.9	1.5e-4	1.23	nss
20	At3g02090	metalloendopeptidase (MPPBETA)	224	59	25	−1.8	2.4e-4	1.26	nss
21	At3g02090	metalloendopeptidase (MPPBETA)	87	17	9	−1.61	6.7e-4	1.20	nss
40	At4g01850	S-adenosylmethionine synthetase 2	92	47	17	2.66	1.3e-9	1.12	nss
41	At5g09810	Actin 7	203	62	23	2.3	4.5e-8	−1.03	nss
42	At5g09810	Actin 7	187	59	22	2.3	5.9e-8	−1.07	nss
43	At3g52930	fructose-bisphosphate aldolase	121	48	13	1.58	5.5e-6	−1.09	nss
44	At1g79550	cytosolic phosphoglycerate kinase	118	55	18	2.62	1.4e-8	−1.04	nss
45	At1g79550	cytosolic phosphoglycerate kinase	132	44	15	3.29	1.2e-10	−1.01	nss
48	At5g40770	prohibitin 3	121	38	11	−1.74	9.8e-5	1.10	nss
49	At3g23400	plastid-lipid associated protein	142	53	14	−1.63	1.9e-6	−1.01	nss
51	At3g23400	plastid-lipid associated protein	106	38	9	−1.58	1.9e-6	1.07	nss
55	At3g16640	translationally controlled tumor protein	93	54	10	2.73	2.2e-10	1.03	nss

[a] Mowse score, for a significant ($p < 0.05$) positive protein identification, cut-off threshold was 71.

[b] Number of peptides matched to the protein sequence.

[c] Ratio represents fold-change of FB1 relative to the control treatment.

[d] Ratio represents fold-change of FB1+ATP relative to FB1 *i.e.* comparison of the FB1+ATP average with the FB1 average to check if ATP addition significantly altered protein response to FB1 alone.

[e] Probability value was replaced by nss when the difference between the treatments being compared was not statistically significant (*i.e.* *p* value >0.05).

FB1 treatment. Other functional categories of FB1-responsive proteins included members of the cell's protein degradation machinery, cytoskeleton-associated proteins with a structural role, and various enzymes involved in several other cellular and metabolic processes.

ATP Synthase β-subunit is a Cell Death Regulator—After identifying eATP-regulated proteins using FB1 treatments and the exogenous ATP filter, we initiated a systematic investigation of their possible role in plant cell death control. From the list of 28 proteins identified in this category, we selected candidates for which *Arabidopsis* transfer-DNA (T-DNA) gene knockout mutants from the SALK T-DNA collection (39) existed. We searched the *Arabidopsis* genome database for gene family members and relegated to the bottom of the list candidates from large gene families, whose function is unlikely to be obtained via reverse genetic studies owing to the high likelihood of gene redundancy. The response of the knockout mutants to FB1 treatment was examined using qualitative and quantitative cell death assays and any mutant with cell death kinetics and phenotype different from wild-type plants clearly defined novel cell death signal regulatory proteins under eATP control.

At the top of our candidate protein list was ATP synthase β-subunit (AT5G08690), a dominant microsomal membrane fraction eATP-regulated protein found in spots 30, 32, 33, and 35–39 (Fig. 2*B*; Table II). Although seven of the spots appeared as a charge train of ~55 kDa, one spot (spot 39) had a lower molecular weight of ~49 kDa (Fig. 2*B*). The same ATP synthase β-subunit protein was identified in the TSP fraction as a ~38 kDa spot (spot 33) (Fig. 2*A*). Distribution of the identified peptides from the two low molecular weight species was predominantly in the central region of the primary sequence of ATP synthase β-subunit (Fig. 3), suggesting the possibility that they arise from N- and/or C-terminal cleavage of the ~55 kDa protein.

We obtained three independent homozygous gene knockout mutants of ATP synthase β-subunit (SALK_005252, SALK_024990, and SALK_135351) with a single T-DNA inserted into predicted exonal regions of the gene (Fig. 4*A*). Gene knockout status was confirmed by RT-PCR. Primers designed to straddle the insertion sites successfully amplified the expected 1795 bp gene-specific product in wild-type Columbia-0 plants whereas the absence of this product in all knockout lines confirmed the lack of a functional copy of the gene (Fig. 4*B*). Next we established the cell death kinetics of leaf tissue obtained from the knockout plant lines against wild-type plant tissues. The assay involves floating leaf discs on FB1 solutions and measuring the conductivity of the solution, which rises as dying cells release their contents. Measured over time, the conductivity profile reflects the relative rates and extent of FB1-induced cell death. The rate and extent of cell death were significantly diminished in all three knockout lines (Fig. 4*C,* 4*E*), indicating that they were resistant to FB1. Leaf discs from the ion leakage assay photographed 96 h post-treatment revealed advanced stages of chlorosis, that accompany cell death, in wild-type tissues (Fig. 4*F*). Corresponding tissues from SALK_135351 and SALK_005252 did not have these symptoms (Fig. 4*F*), displaying the resistance engendered by disruption ATP synthase β-chain subunit gene expression. Moreover, cell death symptom development was also suppressed in the SALK_024990 knockout line when FB1 was infiltrated into leaves left attached to growing plants (Fig. 4*D*). Overall, these results demonstrate that the ATP synthase β-subunit is a novel cell death regulator identified via proteomics.

A

```
  1 MASRRVLSSL LRSSSGRSAA KLVNRNPRLP SPSPARHAAP CSYLLGRVAE
 51 YATSSPASSA APSSAPAKDE GKKTYDYGGK GAIGRVCQVI GAIVDVRFED
101 QEGLPPIMTS LEVQDHPTRL VLEVSHHLGQ NVVRTIAMDG TEGLVRGRKV
151 LNTGAPITVP VGRATLGRIM NVLGEPIDER GEIKTEHYLP IHRDAPALVD
201 LATGQEILAT GIKVVDLLAP YQRGGKIGLF GGAGVGKTVL IMELINNVAK
251 AHGGFSVFAG VGERTREGND LYREMIESGV IKLGEKQSES KCALVYGQMN
301 EPPGARARVG LTGLTVAEYF RDAEGQDVLL FIDNIFRFTQ ANSEVSALLG
351 RIPSAVGYQP TLASDLGALQ ERITTTKKGS ITSVQAIYVP ADDLTDPAPA
401 TTFAHLDATT VLSRQISELG IYPAVDPLDS TSRMLSPHIL GEEHYNTARG
451 VQKVLQNYKN LQDIIAILGM DELSEDDKLT VARARKIQRF LSQPFHVAEI
501 FTGAPGKYVD LKENINSFQG LLDGKYDDLS EQSFYMVGGI DEVVAKAEKI
551 AKESAA
```

B

```
  1 MASRRVLSSL LRSSSGRSAA KLVNRNPRLP SPSPARHAAP CSYLLGRVAE
 51 YATSSPASSA APSSAPAKDE GKKTYDYGGK GAIGRVCQVI GAIVDVRFED
101 QEGLPPIMTS LEVQDHPTRL VLEVSHHLGQ NVVRTIAMDG TEGLVRGRKV
151 LNTGAPITVP VGRATLGRIM NVLGEPIDER GEIKTEHYLP IHRDAPALVD
201 LATGQEILAT GIKVVDLLAP YQRGGKIGLF GGAGVGKTVL IMELINNVAK
251 AHGGFSVFAG VGERTREGND LYREMIESGV IKLGEKQSES KCALVYGQMN
301 EPPGARARVG LTGLTVAEYF RDAEGQDVLL FIDNIFRFTQ ANSEVSALLG
351 RIPSAVGYQP TLASDLGALQ ERITTTKKGS ITSVQAIYVP ADDLTDPAPA
401 TTFAHLDATT VLSRQISELG IYPAVDPLDS TSRMLSPHIL GEEHYNTARG
451 VQKVLQNYKN LQDIIAILGM DELSEDDKLT VARARKIQRF LSQPFHVAEI
501 FTGAPGKYVD LKENINSFQG LLDGKYDDLS EQSFYMVGGI DEVVAKAEKI
551 AKESAA
```

FIG. 3. **ATP synthase β-subunit sequence and sequence coverage.** *A*, sequence coverage by peptides identified from ATP synthase β-subunit in spot 33 (shown in Fig. 2*A*) of the TSP fraction. *B*, sequence coverage by peptides identified from ATP synthase β-subunit in spot 39 (shown in Fig. 2*B*) of the microsomal protein fraction. Residues in bold constitute the trypsin-generated peptides identified by mass spectrometry. Underlined residues form the cleavable predicted mitochondrial targeting sequence.

DISCUSSION

Rationale of using FB1 and an ATP Filter to Identify eATP-regulated Proteins—In order to identify eATP effectors and target proteins, we sought to use an experimental system in which endogenous eATP is depleted so as to trigger changes in the abundance of proteins whose gene expression is tightly regulated by the presence of eATP. This could easily be achieved using enzymatic eATP-sequestering systems such as exogenous apyrase or a glucose/hexokinase mixture. However, we chose to use FB1 treatments, which have been shown to activate progressive depletion of eATP prior to the onset of cell death (5). The advantage of this system is twofold. First, eATP diminishes gradually, which enables the reverse treatment of replenishing eATP in FB1-treated cultures by addition of exogenous ATP. Such a treatment would filter out proteins responding to FB1 only from those responding to FB1-induced eATP removal. Second, FB1 is linked to a physiologically relevant process because it is a pathogen-derived

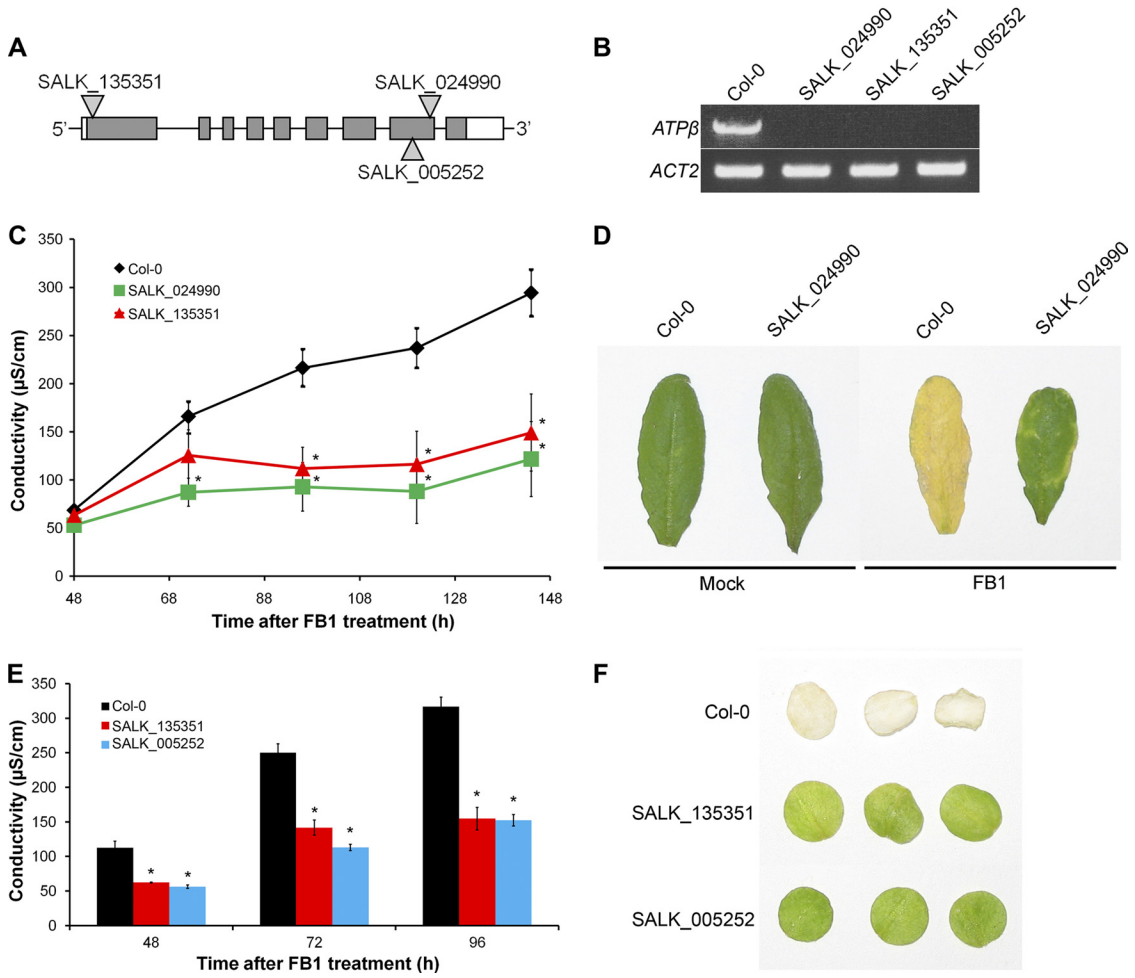

FIG. 4. **ATP synthase β-subunit gene knockout mutant plants are resistant to FB1.** *A*, schematic diagram showing T-DNA insertion sites in three independent knockout mutants (SALK_024990, SALK_135351, and SALK_005252). Inverted triangles indicate insertion sites and gray boxes represent exons. *B*, RT-PCR amplification of *ATP β-synthase subunit* (*ATPase-β*) in RNA samples derived from Columbia-0 (Col-0) plants and the three independent T-DNA insertion mutants. *Actin-2* (*ACT2*) was used as a constitutive reference control. *C,* cell death profiles of leaf disc tissues. Leaf discs were treated with FB1 and incubated in the dark for 48 h and then exposed to light. The conductivity of FB1 solutions on which discs were floating was measured at 48 h and every 24 h thereafter. Values and error bars represent means ± se ($n = 3$). An asterisk indicates data points at which the mutants are significantly ($p < 0.05$) lower that the wildtype (Col-0). *D,* appearance of Col-0 and SALK_024990 leaves 4 days after infiltration with FB1. *E*, leaf disc cell death assay with SALK_135351 and SALK_005252 as described in (*C*). *F*, leaf discs treated as described in (*E*) and photographed at 96 h.

toxin whose use could result in a better understanding of events surrounding cell death processes triggered by certain plant pathogens. Presently it is not clear how endogenous eATP is depleted, but using FB1 can provide clues that may lead to discovery of the mechanism by which pathogens deplete eATP. Because cell cultures treated with FB1 are primed for eATP depletion, we used an excessive concentration of exogenous ATP, as high as 1 mM, to ensure that the FB1-induced eATP deficit was cancelled for the duration of the treatment.

Proteomic Changes Underlying the Switch to FB1-induced Cell Death—There was a clear up-surge in the abundance of molecular chaperones in response to FB1 treatment (Table I and II). This group of proteins is important for maintaining cellular homeostasis by regulating protein folding, assembly, translocation, and degradation (40). Heightened expression of chaperone genes during stress is designed to re-establish normal protein conformation, thereby mitigating the adverse effects of stress (41). Because FB1 activates programmed cell death preceded by a shift in cellular metabolism underpinned by drastic changes in global gene expression, it is not surprising that chaperone proteins are deployed to accommodate the accompanying increased traffic through protein synthesis, translocation and degradation pathways. Not only does FB1 activate cell death processes, but also triggers pathogen defense systems that include synthesis of an array of pathogenesis-related proteins (30), most of which transit through the endoplasmic reticulum and increase the demand for chaperones. Similar chaperone increases occur in *Arabidopsis* responding to programmed cell death-eliciting patho-

gens (42) or exogenous plant hormones (43, 44), which activate enormous changes in the transcriptome. Remarkably, exogenous ATP blocked the rise in chaperone levels, indicating that this response was triggered by the cell death signal depletion of eATP.

Our study has revealed that a prime target for FB1 is cellular ATP synthesis. We identified subunits of the vacuolar and chloroplastic ATP synthase proteins as responsive to FB1, with the great majority belonging to the mitochondrial F_1F_0-ATP synthase machinery. The mitochondrial F_1F_0-ATP synthase has two main parts; the hydrophilic catalytic F_1 complex and the transmembrane proton-transporting F_0 subcomplex. We identified subunits α, β, and δ of the F_1 complex and subunit-D of the F_0 complex. Consistent with our findings, other cell death treatments, such as oxidative stress, have been reported to suppress expression of α-subunit and β-subunit genes (45). Though not determined experimentally in this study, the repression of ATP synthase proteins by FB1 is likely to disrupt oxidative phosphorylation and lead to a significant depression in cellular ATP levels. Harpin, a pathogen-derived cell death-activating elicitor, disrupts oxidative phosphorylation by triggering cytochrome *c* release (46), thereby inhibiting mitochondrial ATP production prior to onset of cell death (46, 47). Reduction in cellular ATP could likely account for growth retardation imposed by FB1 on *Arabidopsis* (5) as general metabolism is slowed. However, the fact that exogenous ATP blocked the suppression of ATP synthase genes by FB1 provides a profoundly fascinating insight. Extracellular ATP appears to positively regulate mitochondrial ATP synthesis, directly linking the cell death trigger—eATP depletion—to the key organelle now established as a central hub for programmed cell death control (48). Thus eATP depletion, driven by FB1 treatment (5), negatively regulates intracellular ATP production, which may lead to decreased ATP secretion that further reduces eATP. This step could serve as a signal amplification loop to ensure the onset of cell death in response to FB1 treatment.

Among the proteins differentially expressed following FB1 treatment were several enzymes involved in protecting cells from oxidative damage. Glutathione transferase and 2-alkenal reductase play significant roles in plant detoxification of lipid peroxide-derived cytotoxic compounds (49, 50). Monodehydroascorbate reductase and dehydroascorbate reductase (Table I) function in the anti-oxidant glutathione-ascorbate cycle (51) whereas thioredoxin (Table I) together with thioredoxin reductase constitute the thioredoxin anti-oxidant system (52). Except for glutathione transferase and 2-alkenal reductase that increased, all the other anti-oxidative enzymes were down-regulated by FB1 (Table I). An overall reduction of these enzymes may account for the observed accumulation of ROS in *Arabidopsis* plants exposed to FB1 (30). ROS can function as signaling molecules (53) or triggers of cell death by attacking membrane lipids to give rise to phytotoxic lipid peroxides (54). Shutdown of some anti-oxidative enzymes and up-regulation of others by FB1 (Table I) could be indicative of a finely tuned balance between harnessing the signaling capability of ROS and tightly controlling their propensity to trigger membrane damage and cell death. Attenuation of FB1 effects on these proteins by exogenous ATP (Table I) implicates them as regulatory or effector elements downstream of eATP signaling in cell death control.

Glycolysis proved to be a major target for FB1 suppression as reflected by seven different proteins belonging to the pathway that were identified as down-regulated proteins (Table I). The reduction in these proteins inevitably constricts flux through the pathway, a strategy that could be useful to divert energy and metabolites toward essential processes required for the response to FB1. For example, up-regulation of components of the amino acid biosynthetic pathways (Table I) could provide building blocks for pathogenesis-related protein synthesis that is triggered by FB1 (30). In addition, slowing down central metabolic pathways could also starve the cells of energy in preparation for programmed cell death. In rescuing the cells from death, exogenous ATP did not attenuate the response of all the glycolytic proteins to FB1, but it enhanced the suppression of some (Table I). This possibly indicates the need for ATP to reset the global metabolic processes in a highly ordered fashion before the full switch back to normal metabolism can be achieved. Reasons for the targeting of glycolytic enzymes by FB1 and exogenous ATP in this study may not be simplistic. It is now known that hexokinase, which catalyzes the first commitment step of glycolysis, is a critical regulator of programmed cell death in plants (55) and animals (56, 57). Glyceraldehyde-3-phosphate dehydrogenase (GAPDH) is now known to translocate to the nucleus of neuronal cells (58) where it activates apoptosis (58, 59). In view of this, a possible role for GAPDH, and the other glycolytic proteins identified in this study, in FB1-induced cell death warrants investigation.

Enzymes of the protein degradation machinery also responded to FB1 treatment (Table I). Changes in protein abundance in response to treatment may entail synthesis of new proteins, for up-regulation, and degradation of existing proteins, for down-regulation. Thus, it is not surprising that the cellular protein degradation machinery was invoked by FB1. A previous study reported that an E3 ubiquitin ligase is a critical regulator of FB1-induced cell death in *Arabidopsis* (60), revealing a crucial function of the ubiquitin-dependent protein degradation pathway in this response. However, an interesting observation is that exogenous ATP did not significantly attenuate the FB1 effects on 4 of the 5 protein spots in this category (Table I). This probably implies that in resetting metabolism from inception of cell death to normal growth metabolism, exogenous ATP requires the action of the protein degradation machinery to eradicate prodeath proteins that had accumulated prior to its addition. Thus, both FB1 and exogenous ATP may recruit the same processes, but for different purposes.

Finally, the rest of the unclassified proteins differentially expressed in response to FB1 reveal that the toxin effects are widespread. The significance of a majority of these proteome changes is not yet clear to us, but when more data on the physiological effects of FB1 on *Arabidopsis* become available in the future, our data sets could prove useful in understanding the basis for FB1 action.

ATP Synthase β-subunit is a Novel Cell Death Signal Regulator—Reverse genetics, using T-DNA insertional mutants from the SALK collection, in combination with FB1 treatments revealed a new role for ATP synthase β-subunit in the regulation of cell death. Although the use of sequence-indexed T-DNA mutants accelerates gene discovery, occasionally the observed phenotype is caused by a secondary mutation and not by the T-DNA-tagged gene indexed in the mutant collection database. Therefore, confirmation of the observed phenotype with either a second independent mutant line or complementation of mutant plants with a copy of the native gene is required (61–63). In this study, we used three independent T-DNA mutant lines and all gave the same phenotype, confirming that ATP synthase β-subunit has a pro-cell death function in *Arabidopsis*.

In two-dimensional gels of microsomal membrane fractions, ATP synthase β-subunit existed as a charge train of seven spots of ~55 kDa and an extra spot (spot 39) of ~49 kDa (Fig. 2*B*). Another ATP synthase β-subunit spot (spot 33) of ~38 kDa was identified in the TSP fraction (Fig. 2*A*). ATP synthase β-subunit has 566 amino acid residues and, according to MitoProt II prediction algorithm (64), the first 38 residues on the N terminus constitute the cleavable mitochondrial targeting sequence. Therefore, the mature sequence with 528 residues has a predicted molecular weight of 54,586.03 Da, which is very close to the experimentally determined molecular weight of ~55 kDa we observed for the charge train (Fig. 2*B*). All the seven ~55 kDa spots in the charge train were down-regulated in response to FB1 whereas the ~38 kDa and ~49 kDa were up-regulated (Tables I and II). The basis for the appearance of these lower molecular weight species is still unclear, but they possibly could arise from proteolytic processing of the ~55 kDa protein spots. If all the amino acids upstream of the identified most extreme N-terminal peptide and downstream of the identified most extreme C-terminal peptide (Fig. 3*A*) were cleaved off from the protein sequence, the predicted size of the truncated sequence becomes ~38.7 kDa, which almost matches the experimentally determined size of the ~38 kDa TSP low molecular weight spot (spot 33, Fig. 2*A*). Doing the same for the ~49 kDa microsomal spot based on the identified peptides (Fig. 3*B*) yields a putative product whose predicted size of ~47.6 kDa is close to the low molecular weight observed on gels (Fig. 2*B*). Therefore, the increase in the abundance of the low molecular weight spots, which is reciprocated by a decrease in the ~55 kDa charge train, could be accounted for by post-translational cleavage of the mature protein. The protein could be proteolytically processed in response to FB1 and ATP treatment protects it from degradation. The respective contribution to cell death regulation of the intact and truncated protein forms and the responsible proteases await further investigation.

The finding that FB1-induced eATP depletion down-regulates the abundance of *Arabidopsis* ATP synthase β-chain subunit agrees with our previous findings in tobacco. Treatment of tobacco with β,γ-methylene adenosine 5′-triphosphate (AMP-PCP), a nonhydrolysable ATP analog that interferes with eATP signaling, causes a dramatic suppression of several subunits of mitochondrial and chloroplast ATP synthase proteins (23). Therefore, eATP depletion achieved by FB1 treatment or by competitive exclusion from its binding sites with excess amounts of AMP-PCP have the same effect on mitochondrial and chloroplast ATP synthase proteins. Given that the γ phosphate of AMP-PCP is recalcitrant to cleavage, we can conclude that eATP-mediated regulation of ATP synthase proteins in *Arabidopsis* may similarly require cleavage of the γ phosphate as in tobacco (23). The nature of this reaction will become clear once the primary eATP target or receptor protein(s) in the extracellular matrix are identified. Although ATP synthase proteins had been identified as eATP-regulated proteins in tobacco (23), we still did not know which eATP controlled physiological processes these proteins mediated. Therefore, in addition to confirming the previous findings in tobacco (23), the current study has now revealed a novel function of the *Arabidopsis* ATP synthase β-subunit in cell death regulation.

The mechanism by which ATP synthase β-subunit promotes death is the focus of current research in our laboratory. Nevertheless, we envisage three possible ways by which ATP synthase β-subunit could perform this function. First, it could directly interact with other core cell death factors in a protein complex that is independent from its classical function in ATP production. This would be similar to cytochrome *c*, a mitochondrial oxidative phosphorylation protein, which translocates to the cytosol, following exposure to a cell death stimulus, and forms a complex with caspase-9 and Apaf-1 to initiate apoptosis (65). Second, ATP synthase β-subunit might be capable of influencing gene expression directly or indirectly, thereby activating cell death genes. Cytosolic proteins such as gluceraldehyde-3-phosphate dehydrogenase (58) and enolase (66) are now known to translocate to the nucleus to affect gene expression, though they are classical glycolytic enzymes. ATP synthase β-subunit could have a similar secondary function in regulation of gene expression as revealed by altered basal expression of several genes in the knockout mutant plants (data not shown). Finally, ATP synthase β-subunit within the F_1 complex could be targeted for direct binding by FB1 or another prodeath protein/signal, leading to an inhibition of mitochondrial ATP production. Likewise, the basis for phytotoxicity of tentoxin, another fungal-derived toxin, is cellular depletion of ATP caused by inhibition of chloroplastic photophosphorylation (67). In this scenario, FB1 resistance

in the At5g08690 knockout mutants could result from the lack of a binding site in the mitochondrial F_1 complex as the target At5g08690 gene product would be absent and replaced by products from one of the two other family members, At5g08680 and At5g08670. The *Arabidopsis* ATP synthase β-subunit protein belongs to a multigene family consisting of three members having 98% sequence similarity at the amino acid level, with differences only in the first 61 amino acids, making this region an ideal focal point for future genetic analyses to determine the basis for its cell death promotional function. Certain residues of the chloroplastic ATP synthase β-subunit were found to be critical for binding of the cell death-inducing tentoxin to the chloroplast F_1-ATP synthase (68). Mutagenesis of a specific chloroplastic ATP synthase β-subunit gene codon of tentoxin-resistant *Chlamydomonas reinhardtii* to match the corresponding codon of tentoxin-sensitive *Nicotiana* species rendered the alga tentoxin-sensitive (68), demonstrating very specific structural requirements for chloroplastic ATP synthase β-subunit function in cell death promotion. Similarly, a single amino acid substitution in the chloroplastic β-subunit switched tentoxin-resistant F_1-ATP synthase of thermophilic *Bacillus* PS3 to a tentoxin-sensitive enzyme (69). A similar situation could account for the nonredundant function of At5g08690 gene product in cell death as revealed by FB1 resistance in the gene knockout plants.

Acknowledgments—We thank Bill Simon and Joanne Robson for help with MALDI-TOF MS analyses.

* This work was supported by BBSRC grant BBH0002831, and a Portuguese government FCT scholarship (SFRH/BD/28814/2006) awarded to D. F. A. T.

S This article contains supplemental Table 1.

§ To whom correspondence should be addressed: School of Biological and Biomedical Sciences, Durham University, Durham DH1 3LE, United Kingdom. Tel.: +44-191-3341253; Fax: +44-191-3341295; E-mail: a.r.slabas@durham.ac.uk.

¶ Both authors contributed equally to this work.

REFERENCES

1. Ivanova, E. P., Alexeeva, Y. V., Pham, D. K., Wright, J. P., and Nicolau, D. V. (2006) ATP level variations in heterotrophic bacteria during attachment on hydrophilic and hydrophobic surfaces. *Int. Microbiol.* **9,** 37–46
2. Ludlow, M., Traynor, D., Fisher, P., and Ennion, S. (2008) Extracellular ATP and ADP mediate Ca^{2+} influx in *Dictyostelium discoideum*. *Purinergic Signalling* **4,** S5–S6
3. Surprenant, A., and Evans, R. J. (1993) ATP in Synapses. *Nature* **362,** 211–212
4. Thomas, C., Sun, Y., Naus, K., Lloyd, A., and Roux, S. (1999) Apyrase functions in plant phosphate nutrition and mobilizes phosphate from extracellular ATP. *Plant Physiol.* **119,** 543–552
5. Chivasa, S., Ndimba, B. K., Simon, W. J., Lindsey, K., and Slabas, A. R. (2005) Extracellular ATP functions as an endogenous external metabolite regulating plant cell viability. *Plant Cell* **17,** 3019–3034
6. Kim, S. Y., Sivaguru, M., and Stacey, G. (2006) Extracellular ATP in plants. Visualization, localization, and analysis of physiological significance in growth and signaling. *Plant Physiol.* **142,** 984–992
7. Zimmermann, H. (2000) Extracellular metabolism of ATP and other nucleotides. *Naunyn-Schmiedebergs Arch. Pharmacol.* **362,** 299–309
8. Housley, G. D., Bringmann, A., and Reichenbach, A. (2009) Purinergic signaling in special senses. *Trends Neurosci.* **32,** 128–141
9. Komoszynski, M., and Wojtczak, A. (1996) Apyrases (ATP diphosphohydrolases, EC 3.6.1.5): Function and relationship to ATPases. *Biochim. Biophys. Acta.* **1310,** 233–241
10. Dichmann, S., Idzko, M., Zimpfer, U., Hofmann, C., Ferrari, D., Luttmann, W., Virchow, C., Jr, Di, Virgilio, F., and Norgauer, J. (2000) Adenosine triphosphate-induced oxygen radical production and CD11b up-regulation: Ca++ mobilization and actin reorganization in human eosinophils. *Blood* **95,** 973–978
11. Pines, A., Perrone, L., Bivi, N., Romanello, M., Damante, G., Gulisano, M., Kelley, M. R., Quadrifoglio, F., and Tell, G. (2005) Activation of APE1/Ref-1 is dependent on reactive oxygen species generated after purinergic receptor stimulation by ATP. *Nucleic Acids Res.* **33,** 4379–4394
12. Resta, V., Novelli, E., Di, Virgilio, F., and Galli-Resta, L. (2005) Neuronal death induced by endogenous extracellular ATP in retinal cholinergic neuron density control. *Development* **132,** 2873–2882
13. North, R. A., and Surprenant, A. (2000) Pharmacology of cloned P2X receptors. *Ann. Rev. Pharmacol. Toxicol.* **40,** 563–580
14. North, R. A. (2002) Molecular physiology of P2X receptors. *Physiol. Rev.* **82,** 1013–1067
15. Demidchik, V., Nichols, C., Oliynyk, M., Dark, A., Glover, B. J., and Davies, J. M. (2003) Is ATP a signaling agent in plants? *Plant Physiol.* **133,** 456–461
16. Jeter, C. R., Tang, W., Henaff, E., Butterfield, T., and Roux, S. J. (2004) Evidence of a novel cell signaling role for extracellular adenosine triphosphates and diphosphates in Arabidopsis. *Plant Cell* **16,** 2652–2664
17. Demidchik, V., Shang, Z. L., Shin, R., Thompson, E., Rubio, L., Laohavisit, A., Mortimer, J. C., Chivasa, S., Slabas, A. R., Glover, B. J., Schachtman, D. P., Shabala, S. N., and Davies, J. M. (2009) Plant extracellular ATP signalling by plasma membrane NADPH oxidase and Ca2+ channels. *Plant J.* **58,** 903–913
18. Foresi, N. P., Laxalt, A. M., Tonón, C. V., Casalongué, C. A., and Lamattina, L. (2007) Extracellular ATP induces nitric oxide production in tomato cell suspensions. *Plant Physiol.* **145,** 589–592
19. Wu, S. J., and Wu, J. Y. (2008) Extracellular ATP-induced NO production and its dependence on membrane Ca^{2+} flux in *Salvia miltiorrhiza* hairy roots. *J. Exp. Bot.* **59,** 4007–4016
20. Reichler, S. A., Torres, J., Rivera, A. L., Cintolesi, V. A., Clark, G., and Roux, S. J. (2009) Intersection of two signalling pathways: extracellular nucleotides regulate pollen germination and pollen tube growth via nitric oxide. *J. Exp. Bot.* **60,** 2129–2138
21. Song, C. J., Steinebrunner, I., Wang, X., Stout, S. C., and Roux, S. J. (2006) Extracellular ATP induces the accumulation of superoxide via NADPH oxidases in Arabidopsis. *Plant Physiol.* **140,** 1222–1232
22. Wu, S. J., Liu, Y. S., and Wu, J. Y. (2008) The signaling role of extracellular ATP and its dependence on Ca-2 flux in elicitation of Salvia miltiorrhiza hairy root cultures. *Plant Cell Physiol.* **49,** 617–624
23. Chivasa, S., Simon, W. J., Murphy, A. M., Lindsey, K., Carr, J. P., and Slabas, A. R. (2010) The effects of extracellular adenosine 5′-triphosphate on the tobacco proteome. *Proteomics* **10,** 235–244
24. Steinebrunner, I., Wu, J., Sun, Y., Corbett, A., and Roux, S. J. (2003) Disruption of apyrases inhibits pollen germination in Arabidopsis. *Plant Physiol.* **131,** 1638–1647
25. Tonón, C., Cecilia, Terrile, M., José, Iglesias, M., Lamattina, L., and Casalongué, C. (2010) Extracellular ATP, nitric oxide and superoxide act co-ordinately to regulate hypocotyl growth in etiolated Arabidopsis seedlings. *J. Plant Physiol.* **167,** 540–546
26. Clark, G., Torres, J., Finlayson, S., Guan, X., Handley, C., Lee, J., Kays, J. E., Chen, Z. J., and Roux, S. J. (2010) Apyrase (nucleoside triphosphate-diphosphohydrolase) and extracellular nucleotides regulate cotton fibre elongation in cultured ovules. *Plant Physiol.* **152,** 1073–1083
27. Tang, W., Brady, S. R., Sun, Y., Muday, G. K., and Roux, S. J. (2003) Extracellular ATP inhibits root gravitropism at concentrations that inhibit polar auxin transport. *Plant Physiol.* **131,** 147–154
28. McAlvin, C. B., and Stacey, G. (2005) Transgenic expression of the soybean apyrase in *Lotus japonicus* enhances nodulation. *Plant Physiol.* **137,** 1456–1462
29. Chivasa, S., Murphy, A. M., Hamilton, J. M., Lindsey, K., Carr, J. P., and Slabas, A. R. (2009) Extracellular ATP is a regulator of pathogen defence in plants. *Plant J.* **60,** 436–448
30. Stone, J. M., Heard, J. E., Asai, T., and Ausubel, F. M. (2000) Simulation of fungal-mediated cell death by fumonisin B1 and selection of fumonisin B1-resistant (fbr) Arabidopsis mutants. *Plant Cell* **12,** 1811–1822

31. Wang, H., Jones, C., Ciacci-Zanella, J., Holt, T., Gilchrist, D. G., and Dickman, M. B. (1996) Fumonisins and *Alternaria alternata lycopersici* toxins: Sphinganine analog mycotoxins induce apoptosis in monkey kidney cells. *Proc. Natl. Acad. Sci. U.S.A.* **93,** 3461–3465
32. Gilchrist, D. G. (1997) Mycotoxins reveal connections between plants and animals in apoptosis and ceramide signaling. *Cell Death Differ.* **4,** 689–698
33. Asai, T., Stone, J. M., Heard, J. E., Kovtun, Y., Yorgey, P., Sheen, J., and Ausubel, F. M. (2000) Fumonisin B1-induced cell death in Arabidopsis protoplasts requires jasmonate-, ethylene-, and salicylate-dependent signaling pathways. *Plant Cell* **12,** 1823–1836
34. May, M. J., and Leaver, C. J. (1993) Oxidative stimulation of glutathione synthesis in *Arabidopsis thaliana* suspension cultures. *Plant Physiol.* **103,** 621–627
35. Chivasa, S., Hamilton, J. M., Pringle, R. S., Ndimba, B. K., Simon, W. J., Lindsey, K., and Slabas, A. R. (2006) Proteomic analysis of differentially expressed proteins in fungal elicitor-treated Arabidopsis cell cultures. *J. Exp. Bot.* **57,** 1553–1562
36. Karp, N. A., Griffin, J. L., and Lilley, K. S. (2005) Application of partial least squares discriminant analysis to two dimensional difference gel studies in expression proteomics. *Proteomics* **5,** 81–90
37. Chivasa, S., Ndimba, B. K., Simon, W. J., Robertson, D., Yu, X. L., Knox, J. P., Bolwell, P., and Slabas, A. R. (2002) Proteomic analysis of the *Arabidopsis thaliana* cell wall. *Electrophoresis* **23,** 1754–1765
38. Oh, S. A., Lee, S. Y., Chung, I. K., Lee, C. H., and Nam, H. G. (1996) A senescence-associated gene of *Arabidopsis thaliana* is distinctively regulated during natural and artificially induced leaf senescence. *Plant Mol. Biol.* **30,** 739–754
39. Alonso, J. M., Stepanova, A. N., Leisse, T. J., Kim, C. J., Chen, H., Shinn, P., Stevenson, D. K., Zimmerman, J., Barajas, P., Cheuk, R., Gadrinab, C., Heller, C., Jeske, A., Koesema, E., Meyers, C. C., Parker, H., Prednis, L., Ansari, Y., Choy, N., Deen, H., Geralt, M., Hazari, N., Hom, E., Karnes, M., Mulholland, C., Ndubaku, R., Schmidt, I., Guzman, P., Aguilar-Henonin, L., Schmid, M., Weigel, D., Carter, D. E., Marchand, T., Risseeuw, E., Brogden, D., Zeko, A., Crosby, W. L., Berry, C. C., and Ecker, J. R. (2003) Genome-wide Insertional mutagenesis of *Arabidopsis thaliana. Science* **301,** 653–657
40. Miernyk, J. A. (1999) Protein folding in the plant cell. *Plant Physiol.* **121,** 695–703
41. Wang, W., Vinocur, B., Shoseyov, O., and Altman, A. (2004) Role of plant heat-shock proteins and molecular chaperones in the abiotic stress response. *Trends Plant Sci.* **9,** 244–252
42. Noël, L. D., Cagna, G., Stuttmann, J., Wirthmüller, L., Betsuyaku, S., Witte, C. P., Bhat, R., Pochon, N., Colby, T., and Parker, J. E. (2007) Interaction between SGT1 and cytosolic/nuclear HSC70 chaperones regulates Arabidopsis immune responses. *Plant Cell* **19,** 4061–4076
43. Schenk, P. M., Kazan, K., Wilson, I., Anderson, J. P., Richmond, T., Somerville, S. C., and Manners, J. M. (2000) Coordinated plant defense responses in Arabidopsis revealed by microarray analysis. *Proc. Natl. Acad. Sci. U.S.A.* **97,** 11655–11660
44. Wang, D., Weaver, N. D., Kesarwani, M., and Dong, X. (2005) Induction of protein secretory pathway is required for systemic acquired resistance. *Science* **308,** 1036–1040
45. Sweetlove, L. J., Heazlewood, J. L., Herald, V., Holtzapffel, R., Day, D. A., Leaver, C. J., and Millar, A. H. (2002) The impact of oxidative stress on Arabidopsis mitochondria. *Plant J.* **32,** 891–904
46. Krause, M., and Durner, J. (2004) Harpin inactivates mitochondria in Arabidopsis suspension cells. *Mol. Plant-Microbe Interact.* **17,** 131–139
47. Xie, Z., and Chen, Z. (2000) Harpin-induced hypersensitive cell death is associated with altered mitochondrial functions in tobacco cells. *Mol. Plant-Microbe Interact.* **13,** 183–190
48. Lam, E. Kato, N., and Lawton, M. (2001) Programmed cell death, mitochondria and the plant hypersensitive response. *Nature* **411,** 848–853
49. Marrs, K. A. (1996) The functions and regulation of glutathione S-transferases in plants. *Annu. Rev. Plant Physiol. Plant Mol. Biol.* **47,** 127–158
50. Mano, J., Belles-Boix, E., Babiychuk, E., Inzé, D., Torii, Y., Hiraoka, E., Takimoto, K., Slooten, L., Asada K., and Kushnir, S. (2005) Protection against photooxidative injury of tobacco leaves by 2-alkenal reductase. Detoxication of lipid peroxide-derived reactive carbonyls. *Plant Physiol.* **139,** 1773–1783
51. Noctor, G., and Foyer, C. H. (1998) Ascorbate and glutathione: keeping active oxygen under control. *Annu. Rev. Plant Physiol. Plant Mol. Biol.* **49,** 249–279
52. Holmgren, A. (1989) Thioredoxin and glutaredoxin systems. *J. Biol. Chem.* **264,** 13963–13966
53. Apel, K., and Hirt, H. (2004) Reactive oxygen species: Metabolism, oxidative stress, and signal transduction. *Ann. Rev. Plant Biol.* **55,** 373–399
54. Montillet, J. L., Chamnongpol, S., Rustérucci, C., Dat, J., van, de, Cotte, B., Agnel, J. P., Battesti, C., Inzé, D., Van, Breusegem, F., and Triantaphylidès, C. (2005) Fatty acid hydroperoxides and H_2O_2 in the execution of hypersensitive cell death in tobacco leaves. *Plant Physiol.* **138,** 1516–1526
55. Kim, M., Lim, J.-H., Ahn, C. S., Park, K., Kim, G. T., Kim, W. T., and Pai, H.-S. (2006) Mitochondria-associated hexokinases play a role in the control of programmed cell death in. *Nicotiana benthamiana. Plant Cell* **18,** 2341–2355
56. Downward, J. (2003) Metabolism meets death. *Nature* **424,** 896–897
57. Majewski, N., Noqueira, V., Bhaskar, P., Coy, P. E., Skeen, J. E., Gottlob, K., Chandel, N. S., Thompson, C. B., Robey, R. B., and Hay, N. (2004) Hexokinase-mitochondria interaction mediated by Akt is required to inhibit apoptosis in the presence or absence of Bax and Bak. *Mol. Cell* **16,** 819–830
58. Saunders, P. A., Chen, R. W., and Chuang, D. M. (1999) Nuclear translocation of glyceralaldehyde-3-phosphate dehydrogenase isoforms during neuronal apoptosis. *J. Neurochem.* **72,** 925–932
59. Ishitani, R., and Chuang, D. M. (1996) Glyceralaldehyde-3-phosphate dehydrogenase antisense oligonucleotides protect against cytosine arabinonucleoside-induced apoptosis in cultured cerebellar neurons. *Proc. Natl. Acad. Sci. U.S.A.* **93,** 9937–9941
60. Lin, S. S., Martin, R., Mongrand, S., Vandenabeele, S., Chen, K. C., Jang, I. C., and Chua, N. H. (2008) RING1 E3 ligase localizes to plasma membrane lipid rafts to trigger FB1-induced programmed cell death in Arabidopsis. *Plant J.* **56,** 550–561
61. Krysan, P. J., Young, J. C., and Sussman, M. R. (1999) T-DNA as an insertional mutagen in Arabidopsis. *Plant Cell* **11,** 2283–2290
62. Tax, F. E., and Vernon, D. M. (2001) T-DNA-associated duplications/translocations in Arabidopsis. Implications for mutant analysis and functional genomics. *Plant Physiol.* **126,** 1527–1538
63. Ajjawi, I., Lu, Y., Savage, L. J., Bell, S. M., and Last, R. L. (2010) Large-scale reverse genetics in Arabidopsis: case studies from the Chloroplast 2010 Project. *Plant Physiol.* **152,** 529–540
64. Claros, M. G., and Vincens, P. (1996) Computational method to predict mitochondrially imported proteins and their targeting sequences. *Eur. J. Biochem*. **241,** 779–786.
65. Li, P., Nijhawan, D., Budihardjo, I., Srinivasula, S. M., Ahmad, M., Alnemri, E. S., and Wang, X. (1997) Cytochrome *c* and dATP-dependent formation of Apaf-1/Caspase-9 complex initiates an apoptotic protease cascade. *Cell* **91,** 479–489
66. Lee, H., Guo, Y., Ohta, M., Xiong, L., Stevenson, B., and Zhu, J. K. (2002) LOS2, a genetic locus required for cold-responsive gene transcription encodes a bi-functional enolase. *EMBO J.* **21,** 2692–2702
67. Steele, J. A., Uchytil, T. F., Durbin, R. D., Bhatnagar, P., and Rich, D. H. (1976) Chloroplast coupling factor 1: A species-specific receptor for tentoxin. *Proc. Natl. Acad. Sci. U.S.A.* **73,** 2245–2248
68. Avni, A., Anderson, J. D., Holland, N., Rochaix, J. D., Gromet-Elhanan, Z., and Edelman, M. (1992) Tentoxin sensitivity of chloroplasts determined by codon 83 of beta subunit of proton-ATPase. *Science* **257,** 1245–1247
69. Groth, G., Hisabori, T., Lill, H., and Bald, D. (2002) Substitution of a single amino acid switches the tentoxin-resistant thermophilic F_1-ATPase into a tentoxin-sensitive enzyme. *J. Biol. Chem.* **277,** 20117–20119